Natural tolerance to transposition is associated with Myc-regulation and DNA repair

Jyoti Lama[1], Satyam Srivastav[1], Sadia Tasnim[1], Donald Hubbard[1] & Erin S. Kelleher[1*]

[1] Department of Biology and Biochemistry, University of Houston

[*] To whom correspondence should be addressed: eskelleher@uh.edu

Abstract

Transposable elements (TE) are mobile genetic parasites whose unregulated activity in the germline causes DNA damage and sterility. In multiple species of *Drosophila, P*-element transposition in larval primordial germ cells (PGCs), as well as adult germline stem cells (GSCs), leads to the loss of both cell types and in extreme cases: agametic gonads. While much is known about the regulation of *P*-element transposition by piRNAs, less is known about tolerance factors that could allow PGCs or GSCs to persist in the face of high transposition rates. Using a panel of highly recombinant inbred lines of *Drosophila melanogaste*r, we identified two linked quantitative trait loci (QTL) associated with natural variation in tolerance to *P*-element transposition. By comparing the total RNA and small RNA pools of multiple tolerant and sensitive genotypes, we found that sensitive genotypes upregulate histones and translational machinery, while tolerant genotypes upregulate chorion proteins. We further observed that sensitive genotypes exhibit increased expression of pericentromeric genes, suggesting reduced heterochromatin formation. Based on these differentially expressed genes and functional classes, location within a QTL, and in-phase single nucleotide polymorphisms (SNPs), we identified two candidate genes that we propose influence tolerance: *brat* and *Nipped-A*. Both candidates are known interactors of the tolerance factor *myc*, a conserved transcription factor whose activity promotes the retention of PGCs that are damaged by *P*-element transposition. *brat* is a translational repressor of *myc*, whereas *Nipped-A* is a co-factor that promotes the expression of genes involved in stem cell self renewal. *Nipped-A* also contributes to double-strand break (DSB) repair as a member of the Tat interactive protein 60-kDa (TIP60) complex, which could promote tolerance by repairing damage caused by transposition. Together our findings reveal complex underpinnings to natural variation in tolerance, including the modulated regulation of stem cell maintenance and DNA repair pathways.

INTRODUCTION

Transposable elements (TE) are mobile DNA sequences that spread through host genomes by replicating in germline cells. Although individual TE insertions are sometimes beneficial, genomic TEs are foremost genetic parasites (reviewed in Chuong et al., 2017). Unrestricted transposition not only produces deleterious mutations, but also double-stranded breaks (DSBs) that lead to genotoxic stress in developing gametes. Generally, hosts avoid the fitness costs of invading parasites, pathogens and herbivores by two distinct mechanisms: resistance and tolerance (Mauricio, 2000; Råberg, 2014; Roy & Kirchner, 2000). Resistance reduces parasite proliferation, whereas tolerant individuals experience reduced fitness costs from parasitism. With respect to TEs, host resistance has been the focus of extensive research, and occurs through production of regulatory small RNAs that transcriptionally and post-transcriptionally silence TEs in the germline (Brennecke et al., 2007; Malone & Hannon, 2009; Nishida et al., 2007). By contrast, tolerance mechanisms that could ameliorate the fitness costs of transposition during gametogenesis remain largely unstudied.

The absence of research on tolerance in part reflects the ubiquity of resistance. For example, in *Drosophila melanogaster*, where resistance to TEs is extensively studied, all actively-transposing TE families are silenced in developing gametes by the Piwi-interacting RNA (piRNA) pathway (Brennecke et al., 2007). In the presence of strong resistance that represses transposition, individual differences in tolerance will not be apparent. Therefore, we make use of the P-M hybrid dysgenesis system in *Drosophila melanogaster*, where resistance to *P*-element DNA transposons is short-circuited in the absence of maternally-transmitted piRNAs (reviewed in Kelleher, 2016). When males bearing genomic *P*-elements (P-strain) are mated to naive females lacking *P*-elements and corresponding piRNAs (M-strain), they produce dysgenic offspring that do not regulate *P*-element transposition in germline cells (Brennecke et al., 2008). A range of fertility effects result from *P*-element induced DNA damage, including the complete loss of germline cells (Kidwell et al., 1977). The ability of an individual to produce gametes despite *P*-element transposition is therefore a measure of tolerance.

Recent forward genetic studies of dysgenic germline loss have revealed potential mechanisms of *P*-element tolerance. Mutations in checkpoint kinase 2 (*chk2*), a key factor in germline response to DSBs, suppresses germline loss in dysgenic females (Moon et al., 2018; Tasnim & Kelleher, 2018). While the gametes produced by the dysgenic females are inviable due to unrepaired DNA damage, these observations suggest that enhanced DSB repair in germline cells could provide tolerance. Alternatively, tolerance could arise by weakening the connection between DNA damage and germline loss, allowing dysgenic individuals to maintain gametogenesis but produce gametes with more mutations. For example, overexpression of the stem cell self-renewal factor *myc* is associated with suppressed germline loss in dysgenic males and females, resulting in the production of additional gametes that exhibit more *P-element* transpositions (Ota & Kobayashi, 2020).

Natural variation in hybrid dysgenesis provides another opportunity to study tolerance. In particular, the degree of dysgenic sterility differs among M-strains, with germline loss being less

prevalent in the offspring of some maternal genotypes (Anxolabéhère et al., 1988; Ignatenko et al., 2015; Kelleher et al., 2018; Kidwell, M.G., Frydryck, T., and Novy, J.B., 1983). This suggests the presence of natural tolerance alleles. Using a panel of highly recombinant inbred lines (RILs) from the Drosophila Synthetic Population Resource (DSPR, King et al., 2012), we recently uncovered a natural tolerance allele through quantitative trait locus (QTL) mapping (Kelleher et al., 2018). We further associated tolerance with reduced expression of *bruno*, a female germline differentiation factor whose ectopic expression in stem cells promotes their loss (Parisi et al., 2001; Wang & Lin, 2007; Xin et al., 2013). We speculated *bruno* tolerance potentially arises by desensitizing gametogenesis to DNA damage in a mechanism analogous to *myc* overexpression.

Here we report results from QTL mapping of hybrid dysgenesis in a second, independent panel of DSPR RILs (Population B, King et al., 2012). We uncovered two QTL peaks close to the second chromosome centromere that determine tolerance to *P*-element activity in young and old females. We further interrogated the tolerance phenotype by contrasting RNA and small RNA expression between tolerant and sensitive genotypes. Finally, we combined information about expression differences, RIL genotypes, and QTL positions to identify novel candidates for natural variation in tolerance.

RESULTS

1. QTL mapping of 2nd chromosome centromere:

The DSPR RILs are all *P*-element free M-strains, which were isolated from natural populations before the *P*-element invasion (King et al., 2012). We therefore screened for tolerant alleles among the panel B RIL genomes by crossing RIL females to males from the reference P-strain Harwich, and examining the morphology of the F1 ovaries (**Figure 1a)**. Atrophied ovaries are indicative of germline loss resulting from *P*-element activity, while non-atrophied ovaries are indicative of tolerance (Kelleher et al., 2018; Schaefer et al., 1979). Since some females exhibit age-dependent recovery from *P*-element hybrid dysgenesis (Khurana et al., 2011), we phenotyped F1 females at two developmental time points: 3 days and 21 days post-eclosion.

Similar to our observations with the Population A RILs (Kelleher et al. 2018), we found continuous variation in the frequency of ovarian atrophy among dysgenic offspring of different RIL mothers, indicating genetic variation in tolerance. Based on a combined linear model of F1 atrophy among 3 and 21 day old females, we estimated the broad-sense heritability of tolerance in our experiment to be ~42.5%. However, the effect of age on the proportion of F1 atrophy was significant but minimal (χ^2= 7.03, df = 1, p-value = 0.008) with 3-day-old females showing only 0.7% increase in atrophy as compared to 21-day-old females. Therefore, age-dependent recovery from dysgenic sterility is not common among the genotypes we sampled.

To identify the genomic regions associated with genetic variation in germline tolerance, we performed QTL analysis using the published RIL genotypes (King et al., 2012). We found a large QTL peak near the 2nd chromosome centromere in both 3 and 21 day-old F1 females **(Figure 1b, Table 1).** However, the intervals of the major QTL peaks, based on the **Δ**2LOD and Bayes Credible Interval (BCI) methods (Lander & Botstein, 1989; Manichaikul et al., 2006), are non-overlapping between the 3 and 21 day-old data sets **(Figure 1c, Table 1)**. The major QTL in 21 day-old females (hereafter, QTL-21d) resides in the euchromatic region and is quite small (990 kb) compared to the major QTL in 3 day-old females (hereafter QTL-3d), which spans the centromere and pericentromeric regions (9.6 Mb). Therefore, there are likely at least two polymorphisms that influence tolerance near the 2nd chromosome centromere, one of which is more important in young 3-day old females, and the other of which is more important in 21 day-old females.

The presence of two tolerance QTL is further supported by the phenotypic classes we detected among founder alleles (B1-B8) for each of the QTL peaks (**Figure 1e**). For QTL-21d, both B2 and B6 founder alleles are sensitive and greatly increase dysgenic ovarian atrophy, while all other founder alleles are tolerant. By contrast for QTL-3d, only the B6 founder allele is associated with increased sensitivity.

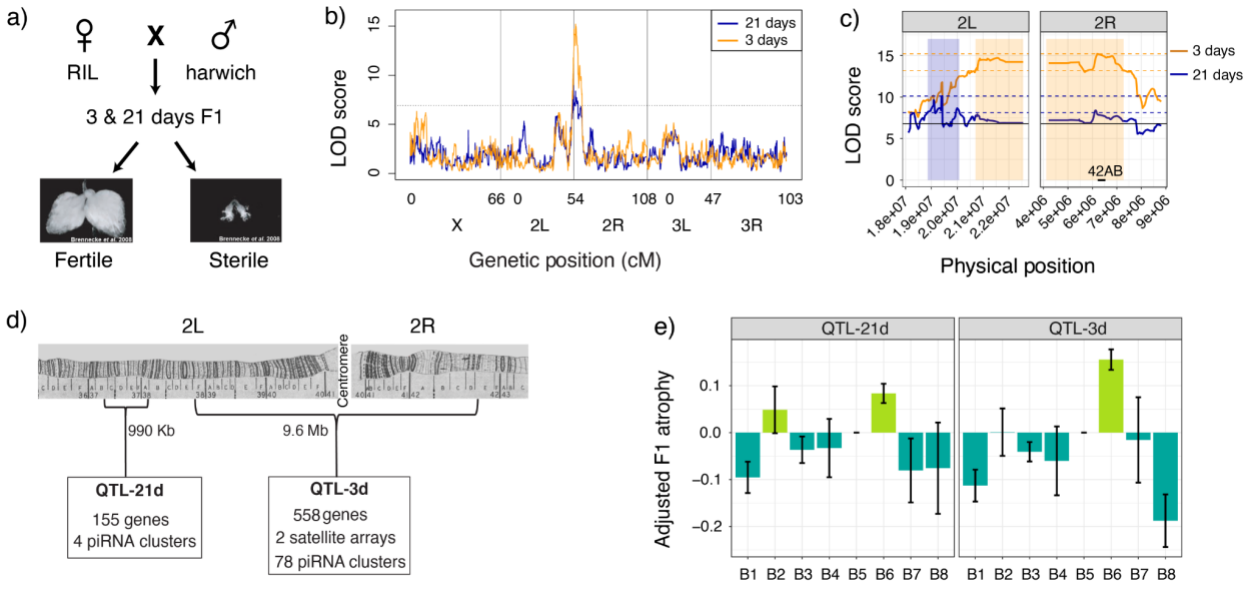

Figure 1: QTL mapping of variation in *P*-element tolerance. **a)** Crossing scheme to phenotype the variation in tolerance to *P*-elements among the RILs by screening for ovarian atrophy in 3 and 21 day-old dysgenic F1 females **b)** The log of odds (LOD) plot for QTL mapping of germline tolerance using 3 day-old (orange) and 21 day-old (blue) F1 females. The dotted line is the LOD threshold and x-axis represents the chromosomal positions. **c)** Zoomed-in figure of QTL mapping from 3 days (orange) and 21 days (blue). The colored boxes show the

Δ2LOD confidence interval of each QTL, and the pairs of dotted lines indicate the LOD peak position and the **Δ**2LOD score that determines the interval. The solid horizontal line is the LOD threshold. **d)** Cytological map depicting the interval of the two QTL peaks (Bridges, 1935; Bridges, 1942). **e)** Graph showing F1 atrophy (y-axis) associated with each of the eight founder alleles (x-axis) at the QTL peaks. All the QTL peaks show 2 phenotypic classes: a sensitive (light green) and tolerant (dark green) class. The data used to generate plot in figure **b**, **c**, and **e** are provided in **Supplemental table S3 and S4**.

Analysis	LOD Score	Peak Position	Δ2LOD CI	BCI	% variation
3-day	15.2	2R:6,192,495	2L:20,710,000-2R:7,272,495	2L:20,820,000-2R:6,942,495	11.13
21-day	10.13	2L:19,420,000	2L:19,170,000-20,080,000	2L:19,010,000-20,000,000	9.78

Table 1: QTL positions for tolerance in 3 and 21-day old females. The peak position, **Δ**2LOD drop confidence interval (**Δ**2LOD CI), and the Bayesian Credible Interval (BCI) in dm6 are provided for each analysis. The data used to identify the LOD peaks and intervals for 3 and 21-day old females can be found in **Supplemental table S3** and **S4**, respectively.

2. Sensitive and tolerant alleles exhibit differential expression of genes involved in chorion formation and chromatin packaging.

Both the QTL regions contain large numbers of protein coding and non-coding RNA genes, piRNA clusters, and repeats, which could influence tolerance (**Figure 1d**). To better understand the tolerance phenotype, we examined differential gene expression between tolerant and the sensitive QTL alleles. We identified three pairs of nearly isogenic lines (NILs), which carried either a sensitive (B6) or tolerant (B4) QTL haplotype across the QTL region (dm6 2L:19,010,000-2R:7,272,495) in otherwise similar genetic backgrounds. We then performed RNA-seq on ovaries of 3-5 day-old females (3 biological replicates). Principal component analysis (PCA) of read counts reveals two independent axes that resolve sensitive and tolerant genotypes, which together account for 40% and 16% of variation (**Figure 2a**). One biological replicate of RIL 21188 (tolerant) was an outlier, which we excluded from our downstream analysis of differentially expressed genes.

We found a total of 530 genes differentially expressed between sensitive and tolerant genotypes (Benjamini-Hochberg adjusted *p*-value <=0.05, fold-change > 1.5). The most significantly enriched GO term among genes upregulated in tolerant genotypes is chorion assembly (Bonferroni corrected *P* value <0.01, **Figure 2b, Supplemental table S7: full report**).

Indeed, all of the major chorion genes were found to be significantly upregulated in the tolerant genotypes (**Figure 2c**, Tootle et al. 2011; Kim et al. 2011). It is unlikely that chorion assembly impacts dysgenic ovarian atrophy, since chorion synthesis occurs in late-stage oocytes (stages 10B-14, G. L. Waring, 2000), whereas atrophy results from the loss of larval primordial germline cells and subsequent germline stem cells (GSCs) (Dorogova et al., 2017; Ota & Kobayashi, 2020; Tasnim & Kelleher, 2018; Teixeira et al., 2017). However, chorion genes reside in clusters that undergo amplification (Claycomb et al., 2004; Spradling, 1981), a process that relies on the efficient repair of DSBs at the boundaries of an amplified region (Alexander et al., 2015). Therefore, upregulation of chorion genes in tolerant genotypes could indicate more efficient DSB repair, which might off-set the impact of *P*-element transposition.

Genes upregulated in the sensitive genotypes are enriched for functions in chromatin assembly and transcription, cell division, and translation. A careful inspection of genes underlying these enriched terms reveals that with the exception of translation, they are majorly driven by the increased expression of replication-dependent (RD) histone gene copies (**Figure 2d**). Overexpression of RD histones is associated with increased sensitivity to DNA damage in yeast (Gunjan & Verreault, 2003; Liang et al., 2012), mice (Murga et al., 2007) and *Drosophila* (Landais et al., 2014; Ozawa et al., 2016). Therefore, histone upregulation exhibited by sensitive alleles may reduce their tolerance to genotoxic stress resulting from *P*-element activity. Notably, the expression of both histone and chorion genes are increased in late oogenesis (Ambrosio & Schedl, 1985; Potter-Birriel et al., 2020; Ruddell & Jacobs-Lorena, 1985; Gail L. Waring, 2000), meaning that their inverted differential expression between sensitive and tolerant genotypes cannot be explained by differential abundance of late stage oocytes.

The *D. melanogaster* histone gene cluster is located the pericentromeric region of QTL-3d and consists of ~100 copies of a 5-kb cluster containing each of the 5 RD histones (*his1, his2A, his2B, his3 and his4)*. However, the differential regulation of histones is unlikely to reflect the presence of a *cis*-regulatory variant within the QTL, since the histone gene cluster is exhibits coordinated and dosage compensated regulation in a unique nuclear body called the histone locus body (HLB; McKay et al., 2015). Rather, we postulated that sensitive and tolerant alleles may differ in heterochromatin formation, since many negative regulators of histone gene transcription are also suppressors of position effect variegation (Su(var), Ner et al., 2002) (Ozawa et al., 2016). In support of this model, sensitive (B6) genotypes exhibit increased expression of pericentromeric genes, as well as genes on the heterochromatic 4th chromosome (**Figure 2e**). We also discovered increased expression of pericentromeric genes associated with the B6 haplotype in a previously published microarray dataset from head tissue (King et al., 2014, **Supplemental figure S1**), suggesting B6 is unusual among the founder alleles in exhibiting reduced heterochromatin formation.

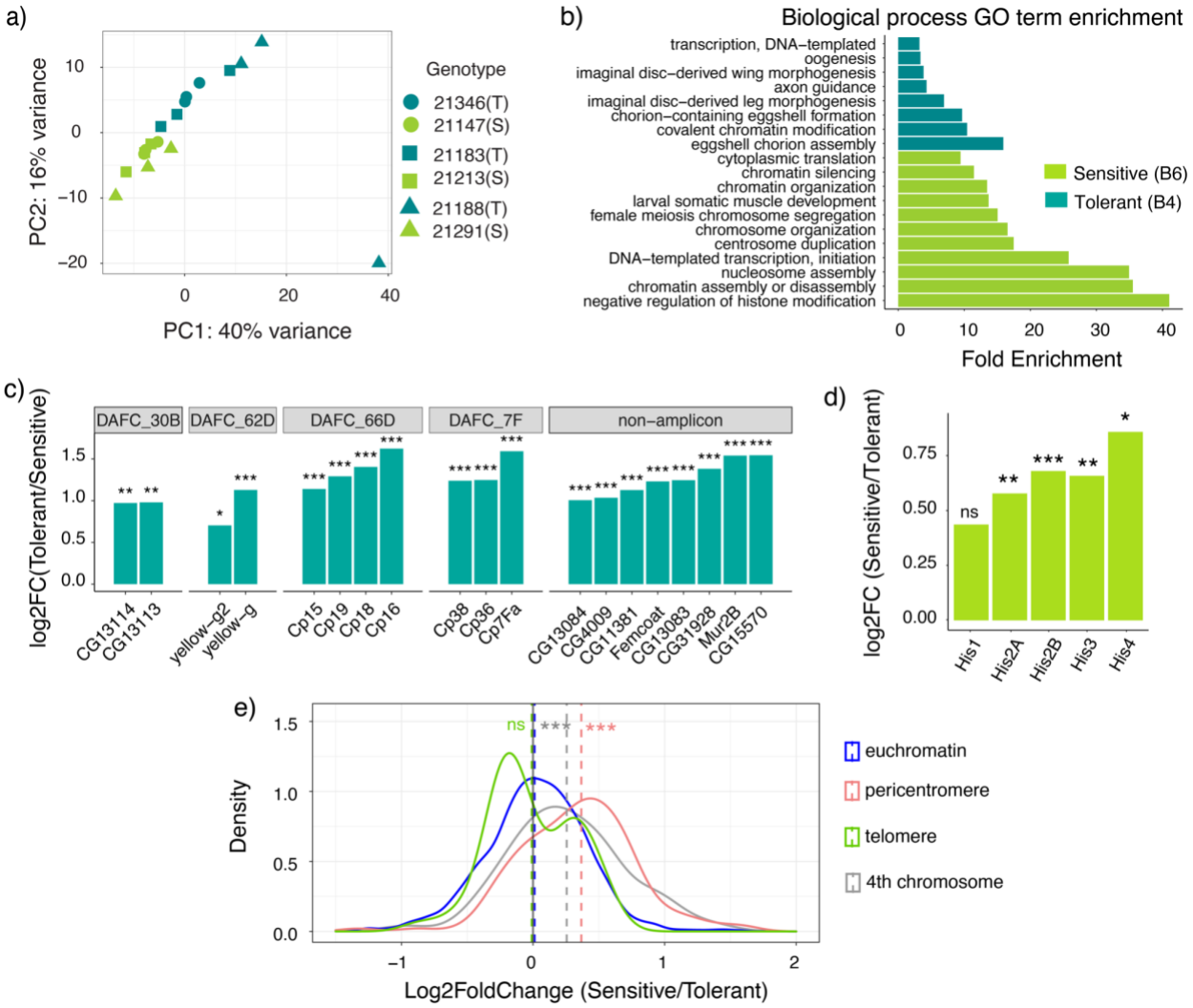

Figure 2: Tolerance is associated with upregulated chorion proteins, whereas sensitivity is associated with upregulated replication-dependent histones. a) PCA analysis of gene expression data of S/sensitive and T/ tolerant genotypes. Members of the same NIL pair are represented by the same shape. **b)** GO terms enriched among genes upregulated in tolerant and sensitive genotypes. **c)** Log2 fold change increase in expression in tolerant genotypes for chorion genes residing in the four amplicons (*Drosophila* Amplicons in Follicle Cells, DAFCs) as well as outside amplicons (Kim et al., 2011; Tootle et al., 2011). **d)** Log2 fold change increase in RD histone expression in sensitive genotypes. **e)**. Probability density plot of log2 fold change values for all euchromatic (blue), pericentromeric (red), telomeric (green) genes and 4th chromosome (gray) between strains carrying sensitive and tolerant alleles. The mean of each distribution is represented by a dotted line. Sensitive genotypes display significantly higher expression of pericentromeric genes (two-sample t-test, t_{141}= -9.32, *p*-value = 2.335e-16) and 4th chromosome genes (two-sample t-test, t_{53} = -4.56, *p*-value = 3.014e-05) when compared to euchromatic genes. For **e**) the x-axis boundaries were confined from (-1.5 to 2) for a better visualization. The pericentromere-euchromatin boundaries were drawn from (Hoskins et al., 2015; Riddle et al., 2011) and subtelomeric-euchromatin boundary coordinates from (Karpen &

Spradling, 1992; Walter et al., 1995; Yin & Lin, 2007). The data represented in panel **a** is provided in **Supplemental table S14** and plot in panel **c, d,** and **e** in **Supplemental table S5**).

3. piRNA clusters in QTL-3d exhibit differential activity that does not translate to TE deregulation.

The pericentromeric region is rich in piRNA clusters, and the QTL-3d region itself harbors 78 piRNA clusters. Particularly, the major piRNA cluster, *42AB,* lies very close (~65kb distal) to the QTL-3d peak position. Although the RIL mothers do not produce or transmit *P*-element-derived piRNAs, the *D. melanogaster* genome harbors more than 100 distinct resident TE families (Kaminker et al., 2002; Quesneville et al., 2005) that are also regulated by piRNAs (Brennecke et al., 2007). If sensitive alleles of piRNA clusters within QTL-3d exhibit reduced silencing of resident (non *P*-element) TEs, resulting transposition could enhance genomic instability triggered by *P*-element activity. We therefore evaluated whether tolerant and sensitive alleles differ in the activity of piRNA clusters using small RNA-seq. A PCA of piRNA cluster expression reveals that sensitive and tolerant genotypes are resolved by the second principal component, accounting for 22% variation in expression (**Figure 3a**).

We did not find evidence that QTL-3d is explained by the differential activity of piRNA cluster *42AB*, as sensitive and tolerant genotypes exhibited comparable piRNA abundances from this locus. Similarly, piRNA abundance from other major piRNA clusters outside the QTL do not differ between sensitive and tolerant alleles (**Figure 3b**). However, we discovered two small pericentromeric piRNA clusters located within QTL-3d that were active in tolerant genotypes but largely quiescent in sensitive genotypes (**Figure 3b, c and d; Supplemental figure S2-3**). While these piRNA clusters contain no annotated TE insertions in the reference genome (dm6), Repbase Censor (Kohany et al., 2006) reveals they are largely composed of TE fragments. The majority (~77%) of these TE fragments are relatively divergent from the consensus (0.65-0.95 sequence similarity; **Supplemental table S9**), and are often most similar to consensus TEs from other (non-*melanogaster*) *Drosophila* species. Given that transpositionally active TE families are often highly similar to the consensus sequence (Bergman & Bensasson, 2007), and piRNA silencing is disrupted by mismatches between the piRNA and its target (Post et al., 2014), this suggests that the differential activity of these two piRNA clusters is unlikely to impact the expression of transpositionally active TEs.

To further evaluate if differences in tolerance are related to resident TE regulation, we compared resident TE expression between sensitive and tolerant genotypes in our RNA-seq data. None of the TE families represented in the QTL piRNA clusters were upregulated in sensitive genotypes (**Figure 3e**). Furthermore, while some TE families are differentially expressed, there is no systematic increase in TE activity in the sensitive genotypes. Rather, more TE families are upregulated in tolerant genotypes (13 TEs) when compared to sensitive (4 TEs) genotypes. Therefore, despite the conspicuous position of QTL-3d surrounding piRNA producing-regions, as well as evidence for differential heterochromatin formation that could impact piRNA biogenesis (**Figure 2b and e**), we find no evidence that tolerance is determined by resident TE silencing.

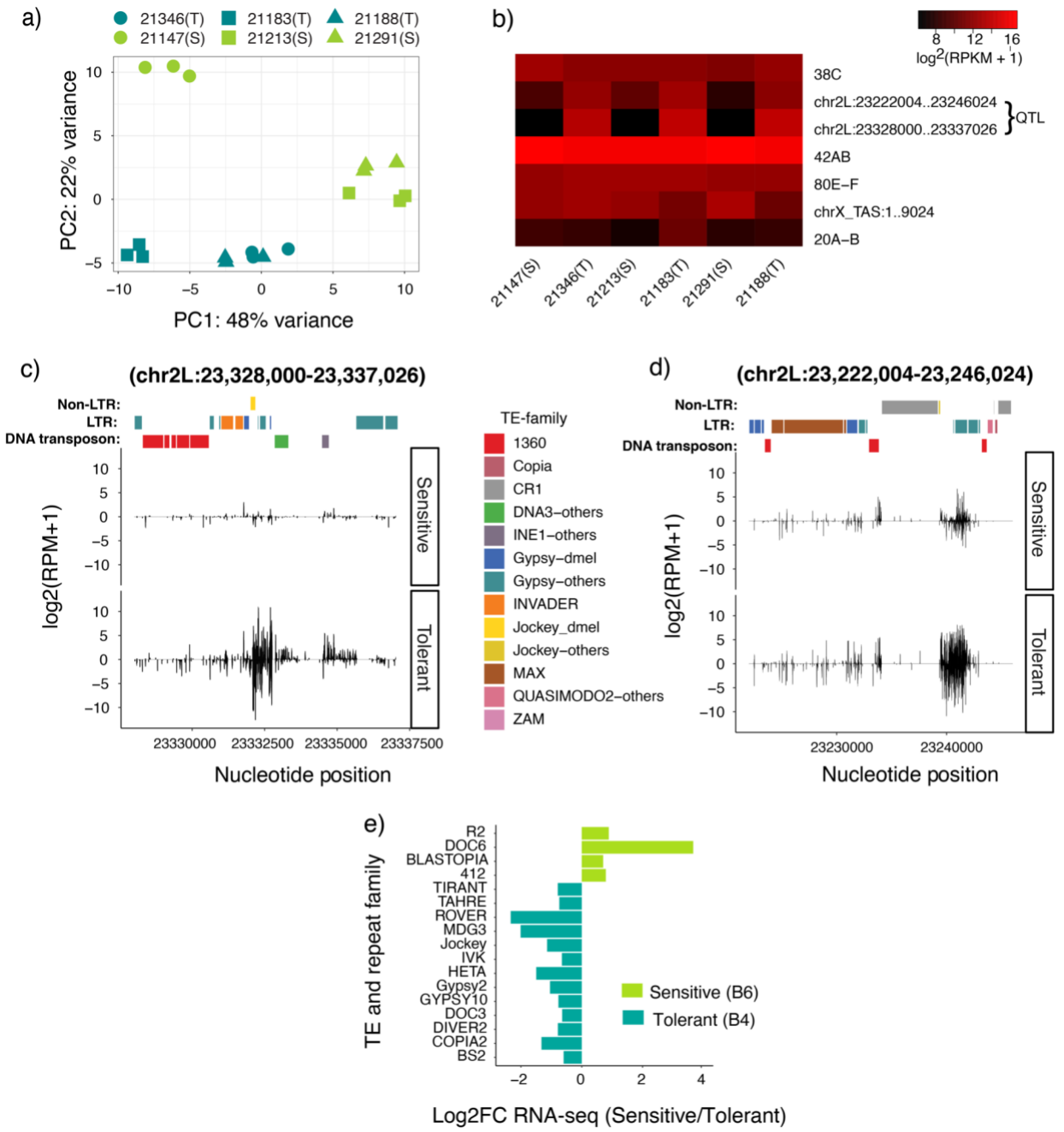

Figure 3: Tolerance is not determined by differential activity of piRNA cluster or TE deregulation. a) PCA analysis for piRNA cluster expression data of S/sensitive and T/ tolerant genotypes. The NIL pairs are represented by the same shapes. **b)** Heat map showing the expression of seven piRNA clusters. NIL pairs that are compared are plotted adjacent to each other. **c and d** represent the piRNA expression between sensitive and tolerant genotypes from one of the NIL pairs along the two QTL piRNA clusters: 2L:23,328,000-23,337,026 and 2L:23,222,004-23,246,024, respectively. Only uniquely mapping piRNAs are considered. The TE families at the top of each figure are represented by different colors. TE-others represent the repeat families coming from sibling species of *D. melanogaster*. Positive value indicates piRNAs

mapped to the sense strand of the reference genome and negative value indicates those from the antisense strand. See **Supplemental figure S2-3** for cluster expression in the remaining NIL pair. For **b, c and d,** piRNA cluster expression levels are estimated by log2 scale transformed of reads per million mapped reads [log2(RPM+1)]. **e)** Bar graph depicting differentially expressed TEs (fold change = 1.5, base mean >= 100, adjusted *p*-value <= 0.05) between sensitive and tolerant genotypes. The data used to plot panel **a** is provided in **Supplemental table S15,** for panel **b** in **Supplemental table S8**, for panel **c** and **d** in **Supplemental table S16 and S9**, and for panel **e** in **Supplemental table S10**)

4. Identifying candidate genes influencing tolerance

In the absence of an obvious role for piRNA clusters within the QTL in determining tolerance, we sought to identify candidate genes that explain the associated phenotypes. We first identified "in-phase" single nucleotide polymorphisms (SNPs), where the genotypic differences among the founder alleles are consistent with their tolerance phenotypes (**Figure 4b**, Long et al., 2014). We identified 64 and 258 genes with in-phase SNPs in QTL-21d and 3d, respectively. These polymorphisms potentially impact either gene expression—by residing within the regulatory/intron region—or affect the activity of the encoded protein through non-synonymous mutations (**Supplemental table S11, S12, and S13**).

To further narrow down the candidates, we similarly identified differentially expressed genes with the QTL. Of 530 genes differentially expressed (**Figure 4a**), 43 are within the QTL, representing an approximately five-fold enrichment in the QTL regions compared to the rest of the genome (Pearson's Chi-squared test, *X-squared* = 255.54, *df* = 1, *p*-value < 2.2e-16, **Figure 4a**). Ultimately, we identified 5 and 14 differentially expressed genes that also carry in-phase SNPs within the QTL-21d and 3d, respectively (**Figure 4c and d**; **Supplemental table 12**). These genes, along with those carrying non-synonymous in-phase SNPs, make up the strongest candidate genes influencing tolerance (**Figure 2b**; **Supplemental table 13**).

We next scoured our list of candidate genes for those with known functions in heterochromatin formation and DNA damage response, whose differential function or regulation are plausibly related to gene expression differences associated with sensitive and tolerant alleles. We similarly looked for genes with known functions in germ cell maintenance or differentiation, which is a critical determinant of the dysgenic phenotype (Ma et al., 2017; Rojas-Ríos et al., 2017; Tasnim & Kelleher, 2018). We found only candidate two genes: *brat* within QTL-21d and *Nipped-A* within QTL-3d, that have functions in determining germ cell fate (Harris et al., 2011; McCarthy et al., 2018). Interestingly, *Nipped-A* is a member of the Tat interacting protein 60 kD (TIP60) complex, which has additional roles in DSB repair and heterochromatin formation (Hanai et al., 2008; Qi et al., 2006; Ruhf et al., 2001; Sinclair et al., 1998). Moreover, we found four other members and interactors of TIP60 complexes that are also upregulated in tolerant genotypes (*dRSF-1/CG8677*, *dom, E(Pc)* & *DMAP1*) (Hanai et al., 2008; Kusch et al.,

2004), and one that is upregulated in sensitive (*yeti*) (Messina et al., 2014). Of these, *yeti* and *dRSF-1* are also located in QTL-3d.

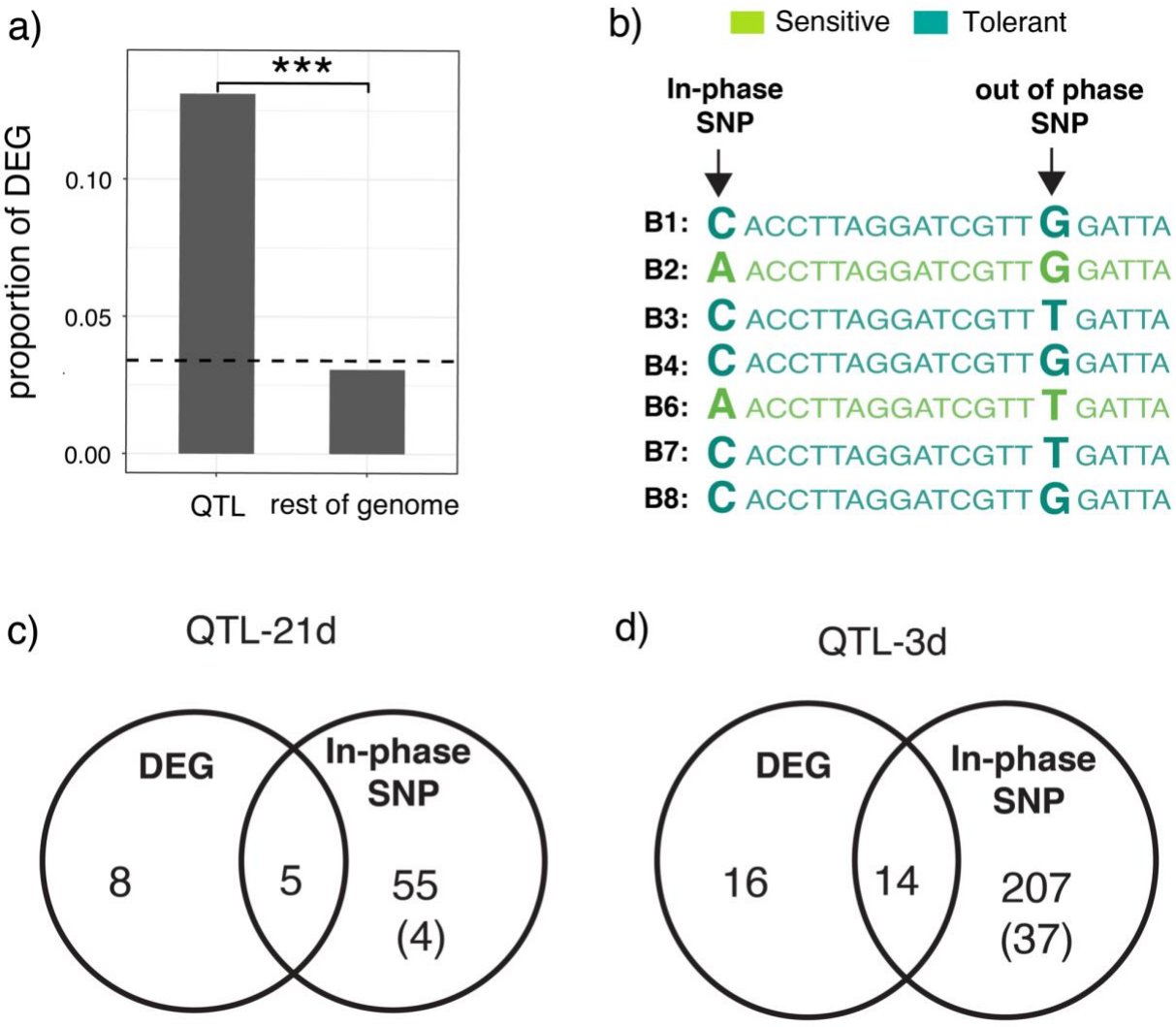

Figure 4: Differential expression and in-phase SNPs identify candidate genes that determine tolerance. a) Bar graph showing enrichment of differentially expressed genes in QTL. The dotted line is the genome wide average. **b)** Schematics representing the in-phase and out of phase SNPs, where each row represents the genotype of the eight B founder strains and the letters in bold indicates SNP alleles. The founders are colored based on their phenotypic classification, either tolerant or sensitive (**Figure 1e**). **c and d)** Venn diagram showing the overlap of differentially expressed genes (DEG) and genes carrying in-phase SNPs for QTL-21d and QTL-3d, respectively. The number within the brackets indicates the genes carrying non-synonymous in-phase SNPs. The data for differential expression of genes for tolerant and sensitive genotypes is provided in **Supplemental table S5**. The data on in-phase polymorphisms for each QTL peak are provided in **Supplemental table S11**. List of candidate

337 genes that have both in-phase polymorphisms and are differentially expressed, and those
338 having non-synonymous in-phase polymorphisms are provided in **Supplemental table S12** and
339 **S13**, respectively.
340
341

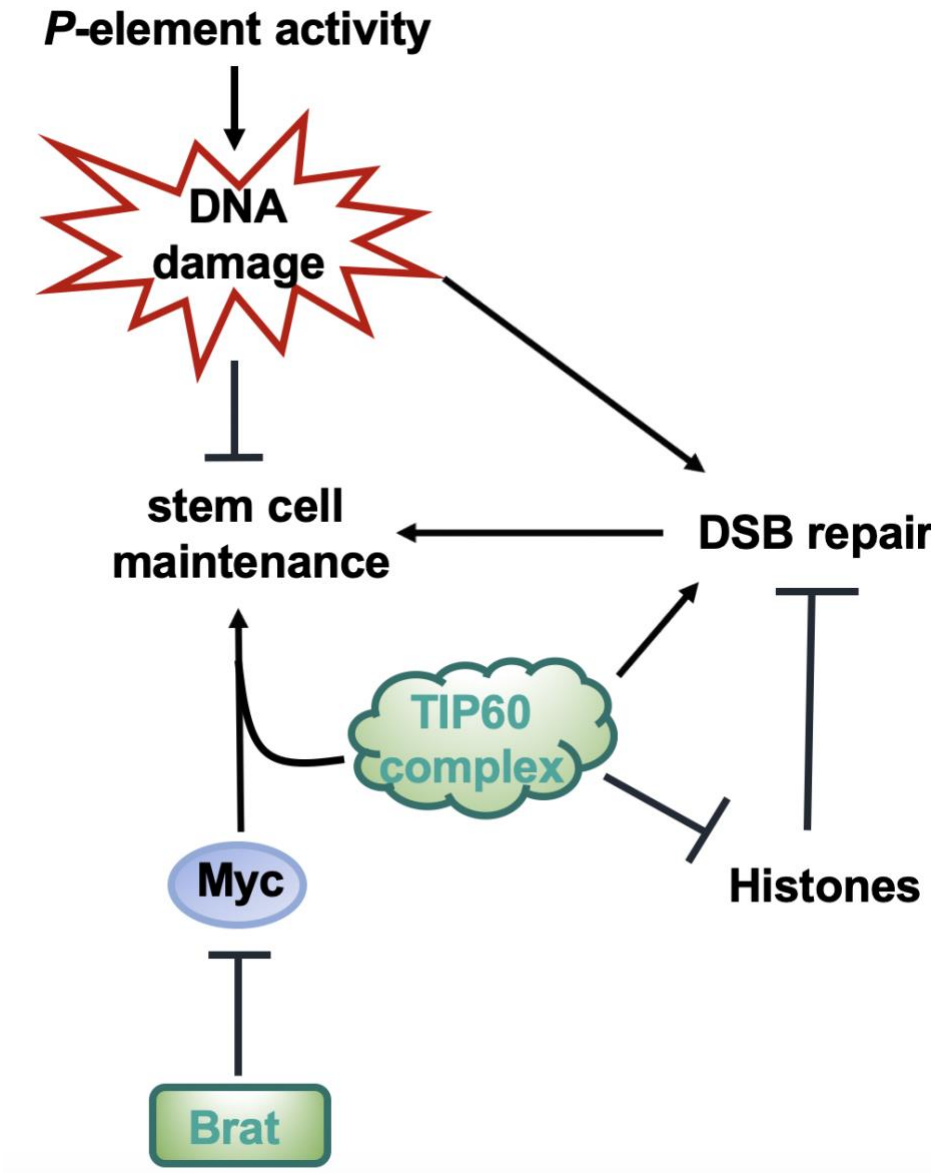

342
343
344 **Figure 5: A model of TE tolerance in Population B RILs.** *brat* and the TIP60 complex
345 (containing Nipped-A) are proposed to determine TE tolerance through the modulation of Myc-
346 dependent stem cell self-renewal or DSB repair (TIP60 only).
347

Discussion

Although small RNA mediated TE regulation is widely studied, little is known about cellular and molecular mechanisms that confer tolerance to transposition. Here we uncovered natural variation in tolerance to *P*-element DNA transposons, which is associated with two or more loci proximal to the second chromosome centromere in *D. melanogaster*. We further showed that tolerant and sensitive genotypes may differ in their ability to form heterochromatin and enact DNA repair, explaining their differential responses to *P*-element transposition. Finally, we identified candidate genes in each QTL that potentially determine the phenotypic differences between tolerant and sensitive alleles. *Nipped-A,* located in QTL-3d, is a member of TIP60 complex and has a non-synonymous in-phase SNP that could alter the activity of encoded protein. By contrast, *brat,* located in QTL-21d, has in-phase SNPs in its intronic and downstream regulatory regions, and is upregulated in the tolerant genotypes.

Nipped-A (QTL-3d) could influence tolerance by promoting the maintenance of larval PGCs or early adult GSCs, which are destabilized by DNA damage (Ma et al., 2016; Ota & Kobayashi, 2020). *Nipped-A* is required for female germ cell maintenance (Yan et al., 2014), as well as maintenance of larval neuroblasts and adult intestinal and male germline stem cells (Prado et al., 2013; Rust et al., 2018; Tauc et al., 2017). While the functional consequences of the non-synonymous SNP that separates tolerant and sensitive *Nipped-A* alleles is not clear, the upregulation of four other TIP60 members (*dRSF-1, dom*, *E(Pc)* & *DMAP1*) suggests increased activity in the tolerant genotypes (**Supplemental table S6**). Reduced expression of pericentromeric genes in tolerant strains also suggests increased TIP60 activity, since TIP60 is involved in heterochromatin formation (Hanai et al., 2008; Qi et al., 2006; Ruhf et al., 2001; Sinclair et al., 1998).

While the specific function of TIP60 in female germ cell maintenance is not clear, TIP60 is a conserved interactor of Myc: a transcription factor with diverse and well-studied roles in tumorigenesis, cell growth and proliferation, cell competition and apoptosis (reviewed in Gallant, 2013; Grifoni & Bellosta, 2015). In larval neuroblasts, TIP60 and Myc coregulate downstream targets that promote stem cell self-renewal (Rust et al., 2018). Similarly, *myc* overexpression confers tolerance in dysgenic larval gonads by suppressing primordial germ cell (PGC) loss (Ota & Kobayashi, 2020). Thus, increased TIP60 function in tolerant genotypes may activate *myc*-dependent tolerance in larvae.

Interestingly, *brat* (QTL 21d) is a translational repressor of *myc* that is upregulated in tolerant ovaries (**Supplemental figure S5 and S12**). Conversely, increased expression of translational machinery suggests increased Myc activity in sensitive ovaries as ribosomal proteins are conserved downstream targets of Myc (**Figure 2B**; Orian et al., 2003). Our data therefore, point to an association between reduced Myc activity and tolerance in adult stages. While puzzling, the impact of Myc activity on cellular persistence is context and cell type specific. For example, reduced Myc activity confers robustness to X-ray induced apoptosis in larval eye imaginal discs, while Myc overexpression in the same tissue induces apoptosis

(Montero et al., 2008). Therefore, the modulation of Myc function over the course of development may be a critical determinant of tolerance, with TIP60-dependent regulation of self-renewal factors increasing tolerance in PGCs, while other Myc targets may decrease tolerance in adults (**Figure 5**). Exploring potential interactions between TIP60, Myc and Brat in determining tolerance presents an enticing avenue for future work.

In addition to promoting germ cell maintenance, *Nipped-A* might also influence tolerance by facilitating repair of DSBs in PGCs or GSCs. The TIP60 complex has a conserved function in DSB repair (Kusch et al., 2004; Sun et al., 2009), and *Nipped-A* in particular promotes the proliferation of intestinal stem cells after DNA damage (Tauc et al., 2017). By contrast, histone upregulation in the sensitive genotypes—which potentially results from reduced TIP60-dependent heterochromatin formation—could inhibit DNA repair. Surplus RD histones are proposed to interfere with DNA-repair machinery, and are considered genotoxic outside of S-phase (Kumar et al., 2020; Landais et al., 2014; Liang et al., 2012). Enhanced repair in tolerant genotypes is further supported by the increased expression of chorion genes, since chorion gene amplification during oogenesis is dependent upon DSB repair (Alexander, Barrasa & Orr-Weaver 2015).

In summary, our work suggests that tolerance to transposition may have a complex architecture, including both the concurrent modulation of Myc-dependent stem cell self renewal and stem cell loss, and the enhanced repair of DSBs. This complexity contrasts our previous study of natural variation in the population A RILs of the DSPR, which uncovered a major effect of the expression of a single differentiation factor, *bruno*, on tolerance (Kelleher et al., 2018). Furthermore, while DNA damage signaling is a clear determinant of dysgenic germ cell loss (Dorogova et al., 2017; Moon et al., 2018; Tasnim & Kelleher, 2018), the potential for natural variation DNA repair to offset the mutagenic effects of transposition has never been evaluated. Our observations therefore point to multiple new mechanisms through which cells could withstand the genotoxic effects of unregulated transposition.

Methods

***Drosophila* Strains and Husbandry.** The recombinant inbred lines (RILs) were generously provided by Stuart Macdonald. Harwich (#4264) was obtained from the Bloomington *Drosophila* stock center. All flies were maintained in standard cornmeal media.

Phenotyping. Phenotyping was performed as described previously in Kelleher *et al* (2018). Briefly, crosses between virgin RIL females and Harwich males were transferred to fresh food every 3-5 days. Since crosses reared at a restrictive temperature (29 ^{o}C) result in complete gonadal atrophy in F1 offspring, we reared our crosses at a lower permissive temperature (25 ^{o}C), which produces an intermediate phenotype that better reveals the variation in severity of dysgenesis (Dorogova et al., 2017; Kelleher et al., 2018; Kidwell et al., 1977; Srivastav & Kelleher, 2017). F1 offspring were maintained for 3 days or 21 days, at which point their ovaries were examined using a squash prep (Srivastav & Kelleher, 2017). 21 day- old females were

transferred onto new food every 5 days as they aged to avoid bacterial growth. Females who produced 1 or more chorionated egg chambers were scored as having non-atrophied ovaries, and females producing 0 egg chambers were scored as having atrophied ovaries.

Crosses and phenotyping were performed for 673 RILs across 22 experimental blocks for 3 day-old F1 females, and 552 RILs across 18 experimental blocks for 21 day-old F1 females. If fewer than 21 F1 offspring were phenotyped for the same cross, it was discarded and repeated if possible. In total, we phenotyped >20 3-day old and 21 day-old F1 female offspring for 595 RILs and 456 RILs, respectively.

QTL mapping. QTL mapping was performed as described in Kelleher *et al.* (2018). Briefly, for each developmental time point, we modeled the arcsine transformed proportion of F1 ovarian atrophy as a function of two random effects: experimental block and undergraduate experimenter. Regression models were fit using the lmer function from the lme4 package (Bates et al., 2015). We then used the residuals as a response for QTL mapping using the DSPRqtl package (King et al., 2012) in R 3.02 (Team & TRDC, 2008). The LOD significance threshold was determined from 1,000 permutations of the observed data, and the confidence interval around each LOD peak was identified by a difference of -2 from the LOD peak position (**Δ**2-LOD), or from the Bayes Confidence Interval (Manichaikul et al., 2006). For **Δ**2-LOD intervals, we took the conservative approach of determining the longest contiguous interval where the LOD score was within 2 of the peak value. We further calculated the broad sense heritability of ovarian atrophy as in Kelleher *et al. (2018)*.

Estimation of Founder Phenotypes and QTL phasing. To estimate the phenotypic effect associated with each founder allele at the QTL peak, we considered the distribution of phenotypes from all RILs carrying the founder haplotype at the LOD peak position (genotype probability >0.95%) (King et al., 2012). QTL were then phased into allelic classes by identifying the minimal number of partitions of founder haplotypes that describes phenotypic variation associated with the QTL peak, as described previously (Kelleher et al., 2018; King et al., 2012).

Identification of in-phase polymorphisms. The SNP data of B founders that used to infer in-phase SNPs is based on dm3 (King et al., 2012). To identify in-phase SNPs we looked for alternate SNP alleles that match the predicted phenotypic class for each of the QTL peaks. For QTL-21d we used the criteria: sensitive class (B2, B6) and the tolerant class (B1, B3, B4, B7, B8), whereas for QTL-3d: sensitive class (B6) and the tolerant class (B1, B2, B3, B4, B7, B8).

Selection of paired RILs with alternate QTL alleles. We identified background matched RILs containing either the B6 (“sensitive”) or B4 (“tolerant”) haplotypes from the start position of the QTL-21d confidence interval (2L: 19,010,000) to the end position of QTL-3d confidence interval (2R: 6,942,495) ($P > 0.9$), based on their published HMM genotypes (King et al., 2012). For all possible RIL pairs (B6 and B4), we then calculated the number of 10 Kb genomic windows in which they carried the same RIL haplotype ($P < 0.9$). We selected three pairs of RILs, which carry the same founder genotype for 47% (21213 & 21183), 46% (21147 & 21346) and 44% (21291 & 21188) of genomic windows outside of the QTL.

Small RNA-seq and total RNA-seq. RILs were maintained at 25°C, and three biological replicates of 20 ovaries were dissected from 3-5 day old females. Ovaries were homogenized in TRIzol and stored at -80°C until RNA extraction. 50 µg of total RNA from each of 18 biological samples (3 biological replicates x 3 pairs) was size fractionated in a 15% denaturing polyacrylamide gel and the 18-30 nt band was excised. 2S-depleted small RNA libraries for Illumina sequencing were then constructed according to the method of Wickersheim and Blumenstiel (2013). Ovarian small RNA libraries were published previously (SRP160954, Zhang & Kelleher, 2019). Ribodepleted and stranded total RNA libraries were generated from the same ovarian samples using NuGen total RNA kit (TECAN). All 18 small RNA and total RNA libraries were sequenced on an Illumina Nextseq 500 at the University of Houston Seq-N-Edit Core.

Small-RNA analysis. Sequenced small RNAs were separated based on size into miRNAs/siRNAs (18-22nt) and piRNAS (23-30nt) (Brennecke et al., 2008). Reads corresponding to contaminating rRNAs, including 2S-rRNA, were removed from each library by aligning to annotated transcripts from flybase (Gramates et al., 2017). To determine the piRNA cluster activity we first uniquely aligned the piRNAs to reference genome (dm6) using Bowtie2 (-v 1 -m 1) (Langmead & Salzberg, 2012). We then used a customized perl script to count reads that mapped to a set of previously annotated piRNA clusters from the same genotypes (497 piRNA clusters, Zhang et al., 2020) Read counts normalized to total mapped microRNAs for each library were used to infer differential expression using DESeq2 (Love et al., 2014) Sliding window estimates of piRNA abundance (Figure 2C,D) were calculated using bedtools genomecov (Quinlan, 2014), normalizing the read counts to total mapped miRNA reads.

Total RNA analysis. Residual ribosomal RNAs (rRNAs) were identified in ribodepleted libraries based on alignment to annotated rRNAs from flybase (Gramates et al., 2017), and excluded from further analysis. Retained reads aligned to the library of consensus satellite and TE sequences from repbase (Bao et al., 2015), plus additional satellite consensus sequences from Larracuente (2014). For TE expression, the total reads mapped to TE sequences were counted using awk commands. Remaining reads that failed to map were aligned to *D. melanogaster* transcriptome (dm6/BDGP6) using Kallisto with default parameters (Bray et al., 2016). Differentially expressed TEs and genes were identified from a combined analysis in DESeq2 (Love et al., 2014). Genes and TEs with base mean >= 100, Adjusted *P*-value <= 0.05 and whose expression pattern differed (fold change >= 1.5) were considered differentially expressed between the B6 and B4 QTL haplotype.

References

Alexander, J. L., Barrasa, M. I., & Orr-Weaver, T. L. (2015). Replication Fork Progression during Re-replication Requires the DNA Damage Checkpoint and Double-Strand Break Repair. *Current Biology: CB*, *25*(12), 1654–1660.

515 Ambrosio, L., & Schedl, P. (1985). Two discrete modes of histone gene expression
516 during oogenesis in Drosophila melanogaster. *Developmental Biology*, *111*(1),
517 220–231.
518 Anxolabéhère, D., Kidwell, M. G., & Periquet, G. (1988). Molecular characteristics of
519 diverse populations are consistent with the hypothesis of a recent invasion of
520 Drosophila melanogaster by mobile P elements. *Molecular Biology and Evolution*,
521 *5*(3), 252–269.
522 Bao, W., Kojima, K. K., & Kohany, O. (2015). Repbase Update, a database of repetitive
523 elements in eukaryotic genomes. *Mobile DNA*, *6*, 11.
524 Bates, D., Mächler, M., Bolker, B., & Walker, S. (2015). Fitting Linear Mixed-Effects
525 Models Using lme4. *Journal of Statistical Software*, *67*(1), 1–48.
526 Bergman, C. M., & Bensasson, D. (2007). Recent LTR retrotransposon insertion
527 contrasts with waves of non-LTR insertion since speciation in Drosophila
528 melanogaster. *Proceedings of the National Academy of Sciences of the United*
529 *States of America*, *104*(27), 11340–11345.
530 Bray, N. L., Pimentel, H., Melsted, P., & Pachter, L. (2016). Near-optimal probabilistic
531 RNA-seq quantification. *Nature Biotechnology*, *34*(5), 525–527.
532 Brennecke, J., Aravin, A. A., Stark, A., Dus, M., Kellis, M., Sachidanandam, R., &
533 Hannon, G. J. (2007). Discrete small RNA-generating loci as master regulators of
534 transposon activity in Drosophila. *Cell*, *128*(6), 1089–1103.
535 Brennecke, J., Malone, C. D., Aravin, A. A., Sachidanandam, R., Stark, A., & Hannon,
536 G. J. (2008). An epigenetic role for maternally inherited piRNAs in transposon
537 silencing. *Science* , *322*(5906), 1387–1392.

538 Bridges, C. B. (1935). SALIVARY CHROMOSOME MAPS: With a Key to the Banding of
539 the Chromosomes of Drosophila Melanogaster. *The Journal of Heredity*, *26*(2), 60–
540 64.
541 Bridges, P. N. (1942). A NEW MAP OF THE SALIVARY GLAND 2L-CHROMOSOME:
542 of Drosophila Melanogaster. *Journal of Heredity*, *33*(11), 403–408.
543 Chuong, E. B., Elde, N. C., & Feschotte, C. (2017). Regulatory activities of transposable
544 elements: from conflicts to benefits. *Nature Reviews. Genetics*, *18*(2), 71–86.
545 Claycomb, J. M., Benasutti, M., Bosco, G., Fenger, D. D., & Orr-Weaver, T. L. (2004).
546 Gene Amplification as a Developmental Strategy: Isolation of Two Developmental
547 Amplicons in Drosophila. *Developmental Cell*, *6*(1), 145–155.
548 Dorogova, N. V., Bolobolova, E. U., & Zakharenko, L. P. (2017). Cellular aspects of
549 gonadal atrophy in Drosophila P-M hybrid dysgenesis. *Developmental Biology*,
550 *424*(2), 105–112.
551 Gallant, P. (2013). Myc function in Drosophila. *Cold Spring Harbor Perspectives in*
552 *Medicine*, *3*(10), a014324.
553 Gramates, L. S., Marygold, S. J., Santos, G. dos, Urbano, J.-M., Antonazzo, G.,
554 Matthews, B. B., Rey, A. J., Tabone, C. J., Crosby, M. A., Emmert, D. B., Falls, K.,
555 Goodman, J. L., Hu, Y., Ponting, L., Schroeder, A. J., Strelets, V. B., Thurmond, J.,
556 & Zhou, P. (2017). FlyBase at 25: looking to the future. *Nucleic Acids Research*,
557 *45*(D1), D663–D671.
558 Grifoni, D., & Bellosta, P. (2015). Drosophila Myc: A master regulator of cellular
559 performance. *Biochimica et Biophysica Acta*, *1849*(5), 570–581.
560 Gunjan, A., & Verreault, A. (2003). A Rad53 kinase-dependent surveillance mechanism

561 that regulates histone protein levels in S. cerevisiae. *Cell*, *115*(5).
562 https://doi.org/10.1016/s0092-8674(03)00896-1
563 Hanai, K., Furuhashi, H., Yamamoto, T., Akasaka, K., & Hirose, S. (2008). RSF
564 Governs Silent Chromatin Formation via Histone H2Av Replacement. *PLoS*
565 *Genetics*, *4*(2). https://doi.org/10.1371/journal.pgen.1000011
566 Harris, R. E., Pargett, M., Sutcliffe, C., Umulis, D., & Ashe, H. L. (2011). Brat Promotes
567 Stem Cell Differentiation via Control of a Bistable Switch that Restricts BMP
568 Signaling. In *Developmental Cell* (Vol. 20, Issue 1, pp. 72–83).
569 https://doi.org/10.1016/j.devcel.2010.11.019
570 Hoskins, R. A., Carlson, J. W., Wan, K. H., Park, S., Mendez, I., Galle, S. E., Booth, B.
571 W., Pfeiffer, B. D., George, R. A., Svirskas, R., Krzywinski, M., Schein, J., Accardo,
572 M. C., Damia, E., Messina, G., Méndez-Lago, M., de Pablos, B., Demakova, O. V.,
573 Andreyeva, E. N., … Celniker, S. E. (2015). The Release 6 reference sequence of
574 the Drosophila melanogaster genome. *Genome Research*, *25*(3), 445.
575 Ignatenko, O. M., Zakharenko, L. P., Dorogova, N. V., & Fedorova, S. A. (2015). P
576 elements and the determinants of hybrid dysgenesis have different dynamics of
577 propagation in Drosophila melanogaster populations. *Genetica*, *143*(6), 751–759.
578 Kaminker, J. S., Bergman, C. M., Kronmiller, B., Carlson, J., Svirskas, R., Patel, S.,
579 Frise, E., Wheeler, D. A., Lewis, S. E., Rubin, G. M., Ashburner, M., & Celniker, S.
580 E. (2002). The transposable elements of the Drosophila melanogaster euchromatin:
581 a genomics perspective. *Genome Biology*, *3*(12), 1–20.
582 Karpen, G. H., & Spradling, A. C. (1992). Analysis of Subtelomeric Heterochromatin in
583 the Drosophila Minichromosome Dp1187 by Single P Element Insertional

584 Mutagenesis. *Genetics*, *132*(3), 737.

585 Kelleher, E. S. (2016). Reexamining the P-Element Invasion of Drosophila

586 melanogaster Through the Lens of piRNA Silencing. *Genetics*, *203*(4), 1513–1531.

587 Kelleher, E. S., Jaweria, J., Akoma, U., Ortega, L., & Tang, W. (2018). QTL mapping of

588 natural variation reveals that the developmental regulator bruno reduces tolerance

589 to P-element transposition in the Drosophila female germline. *PLoS Biology*,

590 *16*(10), e2006040.

591 Kidwell, M.G., Frydryck, T., and Novy, J.B. (1983). The hybrid dysgenesis potential of

592 Drosophila melanogaster strains of diverse temporal and geographical natural

593 origins. *Drosophila Information Service*, *59*, 59–63.

594 Kidwell, M. G., Kidwell, J. F., & Sved, J. A. (1977). Hybrid Dysgenesis in DROSOPHILA

595 MELANOGASTER: A Syndrome of Aberrant Traits Including Mutation, Sterility and

596 Male Recombination. *Genetics*, *86*(4), 813–833.

597 Kim, J. C., Nordman, J., Xie, F., Kashevsky, H., Eng, T., Li, S., MacAlpine, D. M., & Orr-

598 Weaver, T. L. (2011). Integrative analysis of gene amplification in Drosophila follicle

599 cells: parameters of origin activation and repression. *Genes & Development*,

600 *25*(13), 1384.

601 King, E. G., Merkes, C. M., McNeil, C. L., Hoofer, S. R., Sen, S., Broman, K. W., Long,

602 A. D., & Macdonald, S. J. (2012). Genetic dissection of a model complex trait using

603 the Drosophila Synthetic Population Resource. *Genome Research*, *22*(8), 1558–

604 1566.

605 Kohany, O., Gentles, A. J., Hankus, L., & Jurka, J. (2006). Annotation, submission and

606 screening of repetitive elements in Repbase: RepbaseSubmitter and Censor. *BMC*

Bioinformatics, *7*(1), 1–7.

Kumar, K., Moirangthem, R., & Kaur, R. (2020). Histone H4 dosage modulates DNA damage response in the pathogenic yeast Candida glabrata via homologous recombination pathway. *PLoS Genetics*, *16*(3), e1008620.

Kusch, T., Florens, L., Macdonald, W. H., Swanson, S. K., Glaser, R. L., Yates, J. R., Abmayr, S. M., Washburn, M. P., & Workman, J. L. (2004). Acetylation by Tip60 is required for selective histone variant exchange at DNA lesions. *Science* , *306*(5704). https://doi.org/10.1126/science.1103455

Landais, S., D'Alterio, C., & Jones, D. L. (2014). Persistent replicative stress alters polycomb phenotypes and tissue homeostasis in Drosophila melanogaster. *Cell Reports*, *7*(3). https://doi.org/10.1016/j.celrep.2014.03.042

Lander, E. S., & Botstein, D. (1989). Mapping mendelian factors underlying quantitative traits using RFLP linkage maps. *Genetics*, *121*(1), 185–199.

Langmead, B., & Salzberg, S. L. (2012). Fast gapped-read alignment with Bowtie 2. *Nature Methods*, *9*(4), 357–359.

Larracuente, A. M. (2014). The organization and evolution of the Responder satellite in species of the Drosophila melanogaster group: dynamic evolution of a target of meiotic drive. *BMC Evolutionary Biology*, *14*(1), 233.

Liang, D., Burkhart, S. L., Singh, R. K., Kabbaj, M.-H. M., & Gunjan, A. (2012). Histone dosage regulates DNA damage sensitivity in a checkpoint-independent manner by the homologous recombination pathway. *Nucleic Acids Research*, *40*(19), 9604.

Long, A. D., Macdonald, S. J., & King, E. G. (2014). Dissecting Complex Traits Using the Drosophila Synthetic Population Resource. *Trends in Genetics: TIG*, *30*(11),

488.

Love, M. I., Huber, W., & Anders, S. (2014). Moderated estimation of fold change and dispersion for RNA-seq data with DESeq2. *Genome Biology*, *15*(12), 550.

Malone, C. D., & Hannon, G. J. (2009). Small RNAs as guardians of the genome. *Cell*, *136*(4), 656–668.

Manichaikul, A., Dupuis, J., Sen, S., & Broman, K. W. (2006). Poor performance of bootstrap confidence intervals for the location of a quantitative trait locus. *Genetics*, *174*(1), 481–489.

Mauricio, R. (2000). Natural selection and the joint evolution of toleranceand resistance as plant defenses. In *Evolutionary Ecology* (Vol. 14, Issues 4-6, pp. 491–507). https://doi.org/10.1023/a:1010909829269

Ma, X., Han, Y., Song, X., Do, T., Yang, Z., Ni, J., & Xie, T. (2016). DNA damage-induced Lok/CHK2 activation compromises germline stem cell self-renewal and lineage differentiation. *Development* , *143*(23), 4312–4323.

Ma, X., Zhu, X., Han, Y., Story, B., Do, T., Song, X., Wang, S., Zhang, Y., Blanchette, M., Gogol, M., Hall, K., Peak, A., Anoja, P., & Xie, T. (2017). Aubergine Controls Germline Stem Cell Self-Renewal and Progeny Differentiation via Distinct Mechanisms. *Developmental Cell*, *41*(2), 157–169.e5.

McCarthy, A., Deiulio, A., Martin, E. T., Upadhyay, M., & Rangan, P. (2018). Tip60 complex promotes expression of a differentiation factor to regulate germline differentiation in female Drosophila. *Molecular Biology of the Cell*, *29*(24), 2933.

McKay, D. J., Klusza, S., Penke, T. J. R., Meers, M. P., Curry, K. P., McDaniel, S. L., Malek, P. Y., Cooper, S. W., Tatomer, D. C., Lieb, J. D., Strahl, B. D., Duronio, R.

J., & Matera, A. G. (2015). Interrogating the function of metazoan histones using engineered gene clusters. *Developmental Cell*, *32*(3), 373–386.

Messina, G., Damia, E., Fanti, L., Atterrato, M. T., Celauro, E., Mariotti, F. R., Accardo, M. C., Walther, M., Vernì, F., Picchioni, D., Moschetti, R., Caizzi, R., Piacentini, L., Cenci, G., Giordano, E., & Dimitri, P. (2014). Yeti, an essential Drosophila melanogaster gene, encodes a protein required for chromatin organization. *Journal of Cell Science*, *127*(11), 2577–2588.

Montero, L., Müller, N., & Gallant, P. (2008). Induction of apoptosis by Drosophila Myc. *Genesis* , *46*(2), 104–111.

Moon, S., Cassani, M., Lin, Y. A., Wang, L., Dou, K., & Zhang, Z. Z. (2018). A Robust Transposon-Endogenizing Response from Germline Stem Cells. *Developmental Cell*, *47*(5), 660–671.e3.

Murga, M., Jaco, I., Fan, Y., Soria, R., Martinez-Pastor, B., Cuadrado, M., Yang, S.-M., Blasco, M. A., Skoultchi, A. I., & Fernandez-Capetillo, O. (2007). Global chromatin compaction limits the strength of the DNA damage response. *The Journal of Cell Biology*, *178*(7), 1101.

Ner, S. S., Harrington, M. J., & Grigliatti, T. A. (2002). A Role for the Drosophila SU(VAR)3-9 Protein in Chromatin Organization at the Histone Gene Cluster and in Suppression of Position-Effect Variegation. *Genetics*, *162*(4), 1763–1774.

Nishida, K. M., Saito, K., Mori, T., Kawamura, Y., Nagami-Okada, T., Inagaki, S., Siomi, H., & Siomi, M. C. (2007). Gene silencing mechanisms mediated by Aubergine piRNA complexes in Drosophila male gonad. *RNA* , *13*(11), 1911–1922.

Orian, A., van Steensel, B., Delrow, J., Bussemaker, H. J., Li, L., Sawado, T., Williams,

676 E., Loo, L. W. M., Cowley, S. M., Yost, C., Pierce, S., Edgar, B. A., Parkhurst, S.
677 M., & Eisenman, R. N. (2003). Genomic binding by the Drosophila Myc, Max,
678 Mad/Mnt transcription factor network. *Genes & Development*, *17*(9), 1101–1114.
679 Ota, R., & Kobayashi, S. (2020). Myc plays an important role in Drosophila P-M hybrid
680 dysgenesis to eliminate germline cells with genetic damage. *Communications*
681 *Biology*, *3*(1), 185.
682 Ozawa, N., Furuhashi, H., Masuko, K., Numao, E., Makino, T., Yano, T., & Kurata, S.
683 (2016). Organ identity specification factor WGE localizes to the histone locus body
684 and regulates histone expression to ensure genomic stability in Drosophila. *Genes*
685 *to Cells: Devoted to Molecular & Cellular Mechanisms*, *21*(5).
686 https://doi.org/10.1111/gtc.12354
687 Parisi, M. J., Deng, W., Wang, Z., & Lin, H. (2001). The arrest gene is required for
688 germline cyst formation during Drosophila oogenesis. *Genesis* , *29*(4), 196–209.
689 Post, C., Clark, J. P., Sytnikova, Y. A., Chirn, G.-W., & Lau, N. C. (2014). The capacity
690 of target silencing byDrosophilaPIWI and piRNAs. In *RNA* (Vol. 20, Issue 12, pp.
691 1977–1986). https://doi.org/10.1261/rna.046300.114
692 Potter-Birriel, J., Gonsalvez, G. B., & Marzluff, W. F. (2020). A region of Drosophila
693 SLBP distinct from the histone pre-mRNA binding and processing domains is
694 essential for deposition of histone mRNA in the oocyte. In *Cold Spring Harbor*
695 *Laboratory* (p. 2020.04.16.030577). https://doi.org/10.1101/2020.04.16.030577
696 Prado, J. R. M., Srinivasan, S., & Fuller, M. T. (2013). The Histone Variant His2Av is
697 Required for Adult Stem Cell Maintenance in the Drosophila Testis. *PLoS Genetics*,
698 *9*(11), e1003903.

699 Qi, D., Jin, H., Lilja, T., & Mannervik, M. (2006). Drosophila Reptin and Other TIP60
700 Complex Components Promote Generation of Silent Chromatin. *Genetics*, *174*(1),
701 241.
702 Quesneville, H., Bergman, C. M., Andrieu, O., Autard, D., Nouaud, D., Ashburner, M., &
703 Anxolabehere, D. (2005). Combined evidence annotation of transposable elements
704 in genome sequences. *PLoS Computational Biology*, *1*(2), 166–175.
705 Quinlan, A. R. (2014). BEDTools: The Swiss-Army Tool for Genome Feature Analysis.
706 *Current Protocols in Bioinformatics / Editoral Board, Andreas D. Baxevanis ... [et*
707 *Al.]*, *47*, 11.12.1–34.
708 Råberg, L. (2014). How to live with the enemy: understanding tolerance to parasites.
709 *PLoS Biology*, *12*(11), e1001989.
710 Riddle, N. C., Minoda, A., Kharchenko, P. V., Alekseyenko, A. A., Schwartz, Y. B.,
711 Tolstorukov, M. Y., Gorchakov, A. A., Jaffe, J. D., Kennedy, C., Linder-Basso, D.,
712 Peach, S. E., Shanower, G., Zheng, H., Kuroda, M. I., Pirrotta, V., Park, P. J., Elgin,
713 S. C. R., & Karpen, G. H. (2011). Plasticity in patterns of histone modifications and
714 chromosomal proteins in Drosophila heterochromatin. *Genome Research*, *21*(2),
715 147.
716 Rojas-Ríos, P., Chartier, A., Pierson, S., & Simonelig, M. (2017). Aubergine and piRNAs
717 promote germline stem cell self-renewal by repressing the proto-oncogene. *The*
718 *EMBO Journal*, *36*(21), 3194–3211.
719 Roy, B. A., & Kirchner, J. W. (2000). Evolutionary dynamics of pathogen resistance and
720 tolerance. *Evolution; International Journal of Organic Evolution*, *54*(1), 51–63.
721 Ruddell, A., & Jacobs-Lorena, M. (1985). Biphasic pattern of histone gene expression

during Drosophila oogenesis. *Proceedings of the National Academy of Sciences of the United States of America*, *82*(10), 3316–3319.

Ruhf, M. L., Braun, A., Papoulas, O., Tamkun, J. W., Randsholt, N., & Meister, M. (2001). The domino gene of Drosophila encodes novel members of the SWI2/SNF2 family of DNA-dependent ATPases, which contribute to the silencing of homeotic genes. *Development* , *128*(8), 1429–1441.

Rust, K., Tiwari, M. D., Mishra, V. K., Grawe, F., & Wodarz, A. (2018). Myc and the Tip60 chromatin remodeling complex control neuroblast maintenance and polarity in Drosophila. *The EMBO Journal*, *37*(16). https://doi.org/10.15252/embj.201798659

Schaefer, R. E., Kidwell, M. G., & Fausto-Sterling, A. (1979). Hybrid Dysgenesis in DROSOPHILA MELANOGASTER: Morphological and Cytological Studies of Ovarian Dysgenesis. *Genetics*, *92*(4), 1141–1152.

Sinclair, D. A., Clegg, N. J., Antonchuk, J., Milne, T. A., Stankunas, K., Ruse, C., Grigliatti, T. A., Kassis, J. A., & Brock, H. W. (1998). Enhancer of Polycomb is a suppressor of position-effect variegation in Drosophila melanogaster. *Genetics*, *148*(1), 211–220.

Spradling, A. C. (1981). The organization and amplification of two chromosomal domains containing drosophila chorion genes. *Cell*, *27*(1), 193–201.

Srivastav, S. P., & Kelleher, E. S. (2017). Paternal Induction of Hybrid Dysgenesis in *Drosophila melanogaster* Is Weakly Correlated with Both *P* -Element and *hobo* Element Dosage. *G3: Genes|Genomes|Genetics*, g3.117.040634.

Sun, Y., Jiang, X., Xu, Y., Ayrapetov, M. K., Moreau, L. A., Whetstine, J. R., & Price, B.

D. (2009). Histone H3 methylation links DNA damage detection to activation of the tumour suppressor Tip60. *Nature Cell Biology*, *11*(11), 1376–1382.

Tasnim, S., & Kelleher, E. S. (2018). p53 is required for female germline stem cell maintenance in P-element hybrid dysgenesis. *Developmental Biology*, *434*(2), 215–220.

Tauc, H. M., Tasdogan, A., Meyer, P., & Pandur, P. (2017). Nipped-A regulates intestinal stem cell proliferation in Drosophila. *Development* , *144*(4), 612–623.

Team, & TRDC. (2008). The R Project for Statistical Computing. *Http://www.r-Project.org*. https://ci.nii.ac.jp/naid/10027310073

Teixeira, F. K., Okuniewska, M., Malone, C. D., Coux, R.-X., Rio, D. C., & Lehmann, R. (2017). piRNA-mediated regulation of transposon alternative splicing in the soma and germ line. *Nature*, *552*(7684), 268–272.

Tootle, T. L., Williams, D., Hubb, A., Frederick, R., & Spradling, A. (2011). Drosophila Eggshell Production: Identification of New Genes and Coordination by Pxt. *PloS One*, *6*(5), e19943.

Walter, M. F., Jang, C., Kasravi, B., Donath, J., Mechler, B. M., Mason, J. M., & Biessmann, H. (1995). DNA organization and polymorphism of a wild-type Drosophila telomere region. *Chromosoma*, *104*(4), 229–241.

Wang, Z., & Lin, H. (2007). Sex-lethal is a target of Bruno-mediated translational repression in promoting the differentiation of stem cell progeny during Drosophila oogenesis. *Developmental Biology*, *302*(1), 160–168.

Waring, G. L. (2000). Morphogenesis of the eggshell in Drosophila. *International Review of Cytology*, *198*. https://doi.org/10.1016/s0074-7696(00)98003-3

768 Waring, G. L. (2000). Morphogenesis of the eggshells in Drosophila. In *International*
769 *Review of Cytology* (Vol. 198, pp. 67–108). Academic Press.
770 Wickersheim, M. L., & Blumenstiel, J. P. (2013). Terminator oligo blocking efficiently
771 eliminates rRNA from *Drosophila* small RNA sequencing libraries. *BioTechniques*,
772 *55*(5), 269–272.
773 Xin, T., Xuan, T., Tan, J., Li, M., Zhao, G., & Li, M. (2013). The Drosophila putative
774 histone acetyltransferase Enok maintains female germline stem cells through
775 regulating Bruno and the niche. *Developmental Biology*, *384*(1), 1–12.
776 Yan, D., Neumüller, R. A., Buckner, M., Ayers, K., Li, H., Hu, Y., Yang-Zhou, D., Pan,
777 L., Wang, X., Kelley, C., Vinayagam, A., Binari, R., Randklev, S., Perkins, L. A.,
778 Xie, T., Cooley, L., & Perrimon, N. (2014). A regulatory network of Drosophila
779 germline stem cell self-renewal. *Developmental Cell*, *28*(4), 459–473.
780 Yin, H., & Lin, H. (2007). An epigenetic activation role of Piwi and a Piwi-associated
781 piRNA in Drosophila melanogaster. *Nature*, *450*(7167), 304–308.
782 Zhang, S., & Kelleher, E. S. (2019). piRNA-mediated silencing of an invading
783 transposable element evolves rapidly through abundant beneficial de novo
784 mutations. In *bioRxiv* (p. 611350). https://doi.org/10.1101/611350
785 Zhang, S., Pointer, B., & Kelleher, E. S. (2020). Rapid evolution of piRNA-mediated
786 silencing of an invading transposable element was driven by abundant de novo
787 mutations. *Genome Research*, *30*(4), 566–575.

788